Structure and Properties Relationships for Aromatic Polyimides and Their Derived Carbon Membranes: Experimental and Simulation Approaches

ARTICLE *in* THE JOURNAL OF PHYSICAL CHEMISTRY B · NOVEMBER 2005

Impact Factor: 3.3 · DOI: 10.1021/jp050177l · Source: PubMed

Structure and Properties Relationships for Aromatic Polyimides and Their Derived Carbon Membranes: Experimental and Simulation Approaches

Youchang Xiao,[†] Tai-Shung Chung,*[,†] Mei Lin Chng,[†] Shouji Tamai,[‡] and Akihiro Yamaguchi[‡]

Department of Chemical & Biomolecular Engineering, National University of Singapore, Singapore 117602, and Material Science Laboratory, Mitsui Chemicals, Inc., 580-32 Nagaura Sodegaura-City, Chiba 299-0265, Japan

Received: January 11, 2005; In Final Form: July 22, 2005

The main objective of this study is to investigate the factors of the chemical structure and physical properties of rigid polyimides in determining the performance of derived carbon membranes through both the experimental and simulation methods. Four polyimides made of different dianhydrides were pyrolyzed at 550 and 800 °C under vacuum conditions. The resultant carbon membranes exhibit excellent gas separation performances beyond the traditional upper limit line for polymer membranes. The thermal stability and the fractional free volume (FFV) of polyimides were examined by a thermogravimetric analyzer and a density meter. The chain properties of polyimide, such as flatness, chain linearity, and mobility, were simulated using the Cerius[2] software. All above characterizations of polyimides were related to the microstructure and gas transport properties of the resultant carbon membranes. It was observed that the high FFV values and low thermal stability of polyimide produce carbon membranes with bigger pore and higher gas permeability at low pyrolysis temperatures. Therefore, polyimides with big thermally labile side groups should be preferred to prepare carbon membranes at low pyrolysis temperatures for high permeability applications. On the other side, since the flatness and in-plane orientation of precursors may lead carbon membranes to ordered structure, thus obtaining high gas selectivity, linear polyimides with more coplanar aromatic rings should be first choice to prepare carbon membranes at high pyrolysis temperatures for high selectivity applications. The location of the indan group also affects chain flatness and in-plane orientation. As a result, carbon membranes derived from the BTDA-DAI precursor have superior separation performance to those derived from Matrimid.

1. Introduction

Nonporous polymeric membranes have been widely utilized as a commercial gas separation tool for the purification of gaseous mixture to replace the traditional distillation processes which are high cost, energy intensive, and with adverse effect on environment.[1−3] The mechanism of gas transportation through polymeric films involves solution of the gas molecules into the polymeric films followed by solid-phase diffusion.[4] In the past several decades, researchers focused their attention to tailor the chemical structures of polymers in order to simultaneously obtain high gas permeability and permselectivity.[5−7] However, this attempt seems to approach a limit of the tradeoff curve between permeability and selectivity, reported by Robeson[8] and Freeman.[9] Therefore, many researchers switched their interests to inorganic membrane materials, such as zeolite membranes and carbon membranes. The gas separation factors of the two above-mentioned inorganic materials lie above the upper bound of polymers on the tradeoff curve, especially for those gas pairs with similar molecular sizes.[10] Moreover, as compared to polymer materials, inorganic membranes are considered to have higher tolerance to harsh environment due to their sluggish chemical reactivity and better thermal resistance.

In recent years, aromatic polyimides have been extensively used as polymeric precursors of carbon membranes due to their rigid structures and high carbon yields.[11] The film morphology of polyimide as precursors of carbon membranes could be retained very well during high-temperature pyrolysis. A carbon membrane with tailored microstructure derived from the polymeric precursor could be obtained by (1) controlling the pyrolysis conditions, (2) pretreating polymeric precursors, and (3) posttreating carbon membranes. The pyrolysis conditions include the pyrolysis temperature, heating rate, and pyrolysis environment. Geiszler and Koros[12] have reported that an increase in the pyrolysis temperature induced a significant decrease in the permeate flux with a significant increase in selectivity of derived carbon membranes. The lower heating rate required a longer pyrolysis time to make the structure of carbon membrane denser. Moreover, the vacuum pyrolysis increased the selectivity but resulted in less productive membranes than inert purge pyrolyzed membranes. In addition, studies involving modification on polyimide as a precursor of carbon memrbanes have been reported. Kusuki et al.,[13] and Okamoto et al.[14] have thermally treated the polyimide in air before pyrolysis. They showed that the thermostabilization process strengthens the structure of the precursors in order to withstand the high temperature during pyrolysis. Tin et al.[15,16] have proposed another two modifications based on (1) chemical cross-linking and (2) methanol pretreatment on polyimide. The space-filling effects were considered as the main reasons for the alteration of the performance of resultant carbon membranes. On the other hand, some treatments were carried out on carbon membranes after pyrolysis. Koresh and Soffer[17] published the first modifica-

[†] National University of Singapore.
[‡] Mitsui Chemicals, Inc.
* Corresponding author: e-mail chencts@nus.edu.sg; Fax (65)-67791936.

10.1021/jp050177l CCC: $30.25
Published on Web 09/17/2005

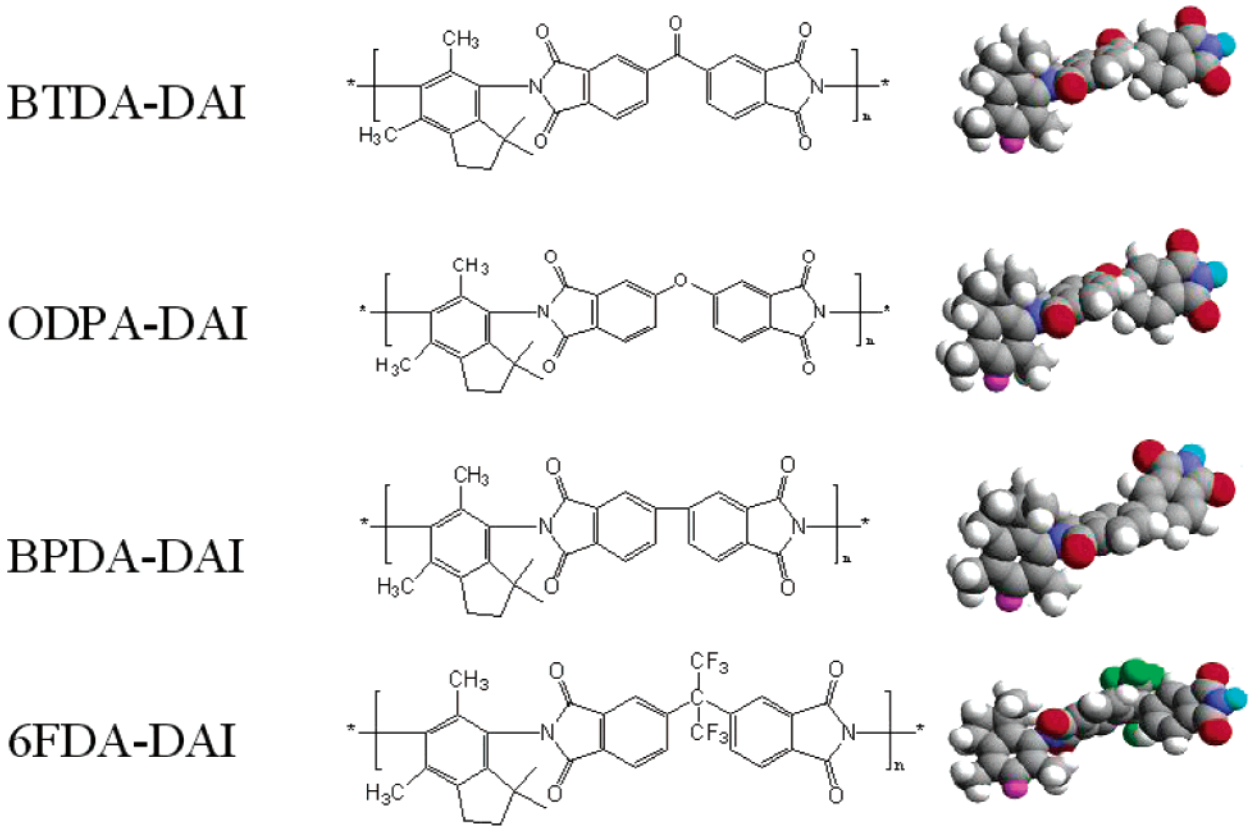

Figure 1. Chemical structures of four polyimides and their simulated three-dimensional conformations.

tion method on carbon membranes, which altered the pore openings by oxidation and sintering. Suda and Haraya[18] explored the modification of carbon membranes by calcining them under a mild activated atmosphere to exhibit excellent selectivity for alkene/alkane separation. Using the methods of chemical vapor deposition and oxidation, Hayashi and co-workers[19] have successfully controlled the pore sizes of carbon membranes and increased the gas separation selectivity.

Since choosing suitable polymer precursors is the first step for preparing carbon membranes, the chemical structure and physical properties of polymer precursors should be primarily considered, although carbonization conditions, pretreatment, and posttreatment are very crucial issues in determining the carbon membrane performance. Nevertheless, there is no publication reported on the effects of different chemical structures of polyimides on the properties of derived carbon membranes, except Park et al.,[20] who have reported that the substitution of methyl groups on polyimides backbone affected the gas permeation properties of the polyimides and their resultant carbon membranes as well. The structure and properties relationship was only discussed from the fractional free volume (FFV) point of view.

The main objective of this study is to investigate the factors of the chemical structure and physical properties of rigid polyimide in determining the performance of derived carbon membranes through both the experimental and simulation methods. Thus, we report the gas permeation properties of carbon membranes from a series of aromatic polyimides synthesized by different dianhydrides. The thermal stability, microstructure, and chain conformation of polyimides were obtained using the thermogravimetric analysis (TGA), wide-angle X-ray diffraction (WAXD), and commercial simulation software Cerius[2]. Moreover, the above characterizations of polyimides were related to the gas permeation properties of the resultant carbon membranes. We believe that this work could provide considerable information for the choice of suitable polyimides in preparing carbon membranes for various targeted applications.

2. Experimental Section

2.1. Materials and Preparation of Polymer Precursor Films. The four polyimides used in this study were synthesized via a generally used a two-step synthesis route through polycondensation reaction of a dianhydride with a diamine. Detailed syntheses about these polyimides from diamine DAI (5,7-diamino-1,1,4,6-tetramethylindan) and corresponding dianhydrides, i.e., 6FDA (2,2′-bis(3,4′-dicarboxyphenyl)hexafluoropropane dianhydride), BTDA (3,3′4,4′-benzophenonetetracarboxylic dianhydride), BPDA (3,3′4,4′-biphenyltetracarboxylic dianhydride), and ODPA (3,3′4,4′-oxydiphthalic dianhydride) have been reported in previous publications.[21−23] The chemical structures of these polyimides are shown in Figure 1. The application of diamines containing an indan group is to increase the solubility of polyimides in solvents.

Before pyrolysis, polyimides were first prepared as dense films. The solutions of less than 2% w/w polyimides in dichloromethane were prepared and filtered using 1 μm filters to remove nondissolved materials and dust particles. The solution was then cast on a leveled clean silicon wafer at room temperature. The polymer films were formed after most of the solvent had evaporated slowly. The nascent films were dried in a vacuum at 250 °C for 48 h to remove the residual solvent. Finally, the membranes films with a thickness about 50 μm were chosen for testing and pyrolysis.

2.2. Preparation of Carbon Membranes. The pyrolysis was performed by a Centurion Neytech Qex vacuum furnace. The pyrolysis temperature of 550 and 800 °C were used in the

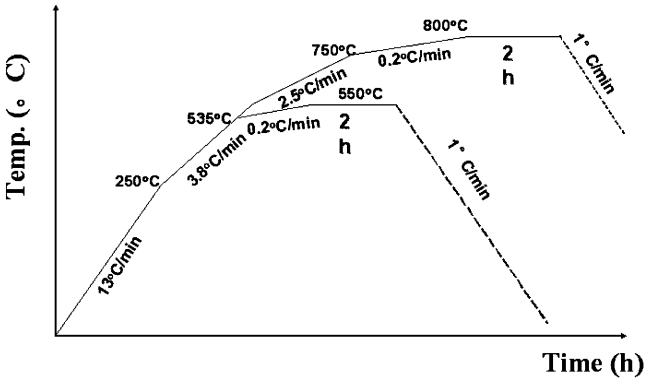

Figure 2. Pyrolysis process to final temperature 550 and 800 °C under vacuum.

preparation of carbon membranes for this study. The detailed pyrolysis protocols are illustrated in Figure 2. The final pyrolysis temperature was reached in several steps. The heating rate was very slow when the temperature is reaching the set value to prevent cracking of carbon membranes. Finally, it was soaked at the final temperature for 2 h. After completing the heating process, membranes were cooled slowly in the vacuum furnace to room temperature and stored in a drybox for further studies. Conveniently, the samples of carbon membranes are named as CM precursor temperature; i.e., the carbon membrane from 6FDA-DAI polyimide at 550 °C is marked as CM-6FDA-550.

2.3. Characterization of Polyimides and Their Derived Carbon Membranes. In a nitrogen environment with a heating rate of 10 °C/min, the thermal properties of polyimides were monitored by a differential scanning calorimetry (DSC) using a Shimadzu 40 type instrument and thermogravimetric analysis (TGA) using a Perkin-Elmer thermogravimetric analyzer as well.

The density of polyimide membranes was calculated on the basis of the Archimedean principles after measuring the weight of the films in air and in ethanol by using a density meter. The fraction of free volume (FFV), which is the ratio of the expansion volume ($V_f = V - V_0$) to the observed specific volume (V), is calculated from the following equation: FFV $= V_f/V = (V - V_0)/V$, where V_0 is chain occupied volume calculated from the van der Waals volume ($V_0 = 1.3V_w$), which can be obtained from the Bondi's group contribution.[24]

Wide-angle X-ray diffraction (WAXD) was performed using a Brukel X-ray diffractometer at room temperature with Cu Kα radiation of wavelength 1.54 Å. The d spacing can be calculated from Bragg's rule as follows: $n\lambda = 2d \sin \theta$, where d is the dimension spacing, θ is the diffraction angle, λ is the X-ray wavelength, and n is an integral number (1, 2, 3, ...).

The chain properties of polyimides also were simulated by Cerius[2] software on SGI (Silicon Graphic Inc.) workstation. Each polyimide chain simulated consists of 50 repeating units so that the system size is enough to represent conformations of a real polymer chain. The initial structures of polyimides were optimized by a molecular mechanics technique. Then a RMMC (the "RIS" Metropolis Monte Carlo method) module within the Cerius[2] for material science was used to calculate the properties of polymer chains, such as the mean-squared end-to-end distance, molar stiffness function, and intrinsic viscosity of the polymer chains.[25] The most advance polymeric force field, pcff (polymer consistent force field), was used for all systems. In addition, van der Waals interactions, electrostatic (Coulombic), and torsion interactions were included in RMMC simulation. During calculations, 100 000 steps were used in the equilibrium portion while 500 000 steps were used in the production portion of the "RIS" Metropolis Monte Carlo simulation.

The degree of in-plane orientation of polyimide films was indirectly demonstrated by a conoscope. Monochromatic, vertically polarized laser light impinges on a polyimide film with 90° of incidence. The phase shift between the normal and the extraordinary light beam behind the polyimide film is recorded. The incident linearly polarized wave can be regarded as the superimposition of two "in-phase" oscillating waves which are polarized, one perpendicular and the other parallel to the in-plane orientation direction. The two light waves pass through the film at different speeds, inducing a phase difference. If the corresponding refractive indices are designated by n_{a0} and n_0, l is the distance in the film covered by the light, and then there is a difference in optical paths for the two waves of $l(n_{a0} - n_a)$. This corresponds to a phase displacement of $\Delta = 2\pi(l/\lambda)(n_{a0} - n_0)$, where λ is the wavelength of the light. The luminous intensity I behind the analyzer is obtained when the polarizer and the analyzer are crossed and the light pass through the polyimide film. I_0 is the luminous behind the analyzer when the polarizer and the analyzer are aligned in the same direction, and there is no film in the sample holder. The relationship between these two values is $I = I_0 \sin^2(\Delta/2)$. Therefore, we can achieve the phase shift value Δ from $\Delta/2 = \arcsin\sqrt{I/I_0}$. Comparison between the Δ of different polyimide films may tell us the relative degree of in-plane orientation of these polyimides.

CO_2 sorption tests were conducted for carbon membranes using a Cahn D200 microbalance sorption cell. The microbalance was first calibrated with the gas as a function of pressure. Then ~200 mg of the film materials was placed on the sample pan, following by evacuation for 24 h. As gas at a specific pressure was fed into the system, the sample started to adsorb the gas until the equilibrium was achieved. From the weight gain, the amount of gas dissolved in the material was calculated after accounting for the buoyancy correction.

The pure gas permeabilities (in barrers, 1 barrer $= 1 \times 10^{-10}$ cm^3 (STP) cm/(cm^2 s cmHg)) of O_2, N_2, CO_2, and CH_4 were measured using a constant-volume method. The testing temperature and pressure was 35 °C and 10 atm, respectively. The details of apparatus design and testing procedures have been reported elsewhere.[26] The ideal selectivity is determined from $\alpha_{A/B} = P_A/P_B$.

3. Results and Discussion

3.1. Characterization of Polyimides. The glass transition temperatures (T_g) of all polyimides were undetectable in the temperature range from 100 to 500 °C. Melting temperatures (T_m) of these polyimides were also unable to be observed by the endothermic transition of DSC measurements. This indicates that the intrasegmental motion of these polyimide chains is highly restricted due to the rigid imide linkages. As a result, these polyimides should be considered as suitable precursors for carbon membranes, since the film structure can be maintained during pyrolysis process.

As shown in Figure 3, thermal gravimetric analysis (TGA) was used to examine the thermal decomposition kinetics and stability of polyimides under nitrogen purge. The thermal stability is compared by the T_d^5 values of these polyimides which indicate the temperature where the samples encountered 5% weight loss. All polyimides are stable up to ~500 °C. The 6FDA-DAI and BTDA-DAI polyimides decompose earlier at around 530 °C, as compared to the T_d^5 of BPDA-DAI polyimide at 570 °C. 6FDA-DAI polyimide loses about 65 wt % when the temperature reaches 800 °C, while BTDA-DAI and ODPA-DAI polyimide lose about 50 wt % at the same temperature.

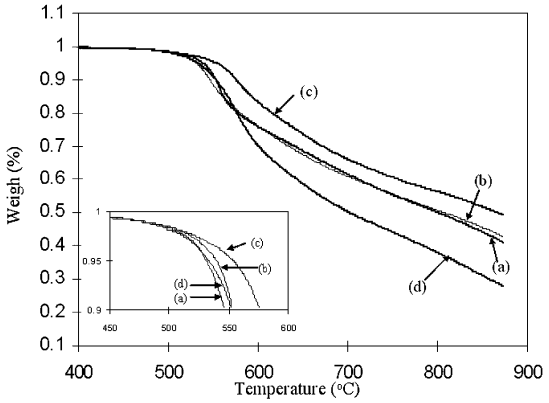

Figure 3. TGA curves for four polyimides as the precursors of carbon membranes: (a) BTDA-DAI, (b) ODPA-DAI, (c) BPDA-DAI, and (d) 6FDA-DAI.

TABLE 1: Physical Properties of Polyimides Precursors

polyimides	density	FFV	*d* spacing (Å)
BTDA-DAI	1.2251	0.1541	5.74
ODPA-DAI	1.2183	0.1641	5.89
BPDA-DAI	1.1902	0.1676	6.00
6FDA-DAI	1.3263	0.1701	7.02

TABLE 2: Gas Permeation of Polyimides Membranes (10 atm and 35 °C)

	permeability (barrer)				ideal selectivity	
	O_2	N_2	CH_4	CO_2	O_2/N_2	CO_2/CH_4
BTDA-DAI	37.2	8.52	8.12	140.4	4.34	17.28
ODPA-DAI	43.9	10.3	10.3	161.1	4.26	15.60
BPDA-DAI	83.4	22.0	23.9	328.8	3.79	13.73
6FDA-DAI	198.2	58.6	50.5	692.3	3.38	13.72

Among all polyimides, the BPDA-DAI polyimide shows the highest thermal stability and the highest carbon yields. A possible reason for the lower thermal stability of 6FDA-DAI and BTDA-DAI polyimides is that the fluorine and oxide atoms in the side groups can easily decompose as gases and expel from the polymer matrix, but the BPDA-DAI polyimide does not contain such non-carbon atoms in the side groups. Moreover, between 550 and 600 °C, the rates of weight loss for all polyimides reach the maximum. After 700 °C, the rates of weight loss decrease and become almost identical for all polyimides. It may be evident that there are two different degradations during the whole pyrolysis process.

The physical properties of these polyimides are given in Table 1. It can be seen that the FFV value for four polyimides is in the following order: BTDA-DAI < ODPA-DAI < BPDA-DAI < 6FDA-DAI. The *d* spacing data obtained from WAXD also consistent with this sequence. The gas permeability coefficients of these polyimide films measured at 35 °C and 10 atm are summarized in Table 2. It is clear that the gas permeabilities change follows the sequence of FFV values and *d* spacing. The higher FFV and *d* spacing indicate the looser interchain structure. Therefore, more free spaces in films induce higher gas permeability but lower ideal selectivity. Interestingly, the gas permeation of 6FDA-DAI is almost double that of the BPDA-DAI polyimide; the selectivity coefficients, however, are quite close. This may be due to the 6FDA bulky group on the polymer backbone, which inhibits chain packing and hinders segmental motion.[27]

3.2. WAXD Patterns for Carbon Membranes and Polyimides as Their Precursors. Ideally, Bragg's rule has been used to determine the interchain distance (*d* spacing) in the amorphous polymers by measuring the maximum intensity in the broad-band region. In addition, X-ray diffraction is a useful tool for studying the organization of carbon at the molecular level. Wide-angle X-ray diffraction data are shown in Figure 4 to characterize the average *d* spacing of 6FDA-DAI polyimide and its derived carbon membranes under 550 and 800 °C pyrolysis temperatures. When the polyimide was pyrolyzed at a temperature of 550 °C, the spectra of carbon material show a new broad peak at a *d* spacing around 3.8−4.0 Å, while the peak around 5.0−6.0 Å still exists with weaker intensity compared to the spectra of polyimide as its precursor. The appearance of new peak at 3.8−4.0 Å implies that a new carbon structure is constructed during pyrolysis process. But this structure is still far from graphite crystal, since the spacing of parallel graphite layers of graphite, d_{002} should be 3.35 Å. The conservation of peak around 5.0−6.0 Å indicates that carbon membranes pyrolyzed under low temperatures still maintain similar amorphous structure as their precursors. When the polyimide is pyrolyzed to 800 °C, another new peak at 2.1 Å is observed in the diffraction pattern of resultant carbon membranes. The peak at 2.1 Å could be pointed to the *d* spacing of graphite (100) plane, which represents the repeated aromatic ring in graphitic structure. In addition, the peak around 3.8−4.0 Å moves to smaller *d* spacing range of 3.6−3.8 Å, and its intensity is also strengthened, after the high-temperature pyrolysis. This distance is still bigger than the spacing of parallel graphite layers in graphitic crystal. Therefore, we can conclude that the monolayer graphite sheets should be formed in carbon membranes during high-temperature pyrolysis, and the structure of carbon membranes tends to approach the graphic crystal state.

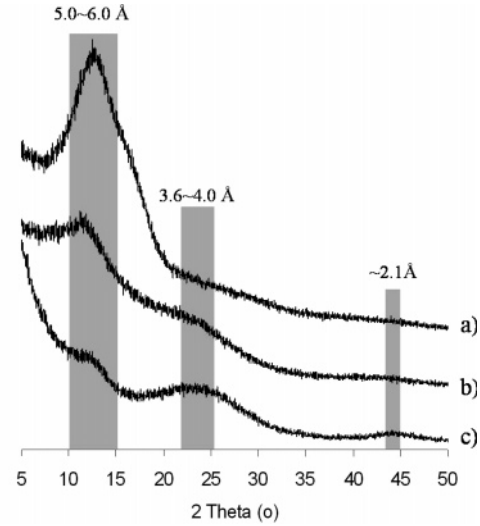

Figure 4. Comparison of WAXD patterns for polyimide and carbon membranes: (a) 6FDA-DAI polyimide, (b) CM-6FDA-550, and (c) CM-6FDA-800.

The TGA and WAXD results suggest that the pyrolysis process of polyimide films consists of two processes, i.e., carbonization at a low-temperature range of 500−700 °C and graphitization at a high temperature of pyrolysis (>700 °C). In the carbonization processes, the most weight loss of polyimides is induced by the expelling of noncarbon atoms as different gases. The rates of weight loss are related to the chemical structures of polyimide. However, the chain conformation of carbonized materials will be retained as that of polyimide in the carbonization process. When the pyrolysis temperature increases up to 700 °C, the linkage of independent aromatic rings is induced by dehydrogenization and denitrogenization. As the result, the amorphous carbon will move toward to the graphitic state which is more thermodynamically stable.

TABLE 3: Simulated and Experimental Results of Chain Properties for Four Polyimides

	BTDA-DAI	ODPA-DAI	BPDA-DAI	6FDA-DAI
dihedral angle (deg)	58.5	66.0	40.1	76.9
mean-squared end-to-end distance ($Å^2$)	23403	19510	27047	15512
molar stiffness function ($g^{0.25}$ $cm^{1.5}/mol^{0.75}$)	236	205	260	183
intrinsic viscosity (cm^3/g)	36.5	28.47	48.1	15.77
phase shift of polarized light passed through (Δ)	0.12	0.09	0.42	0.07

3.3. A Molecular Simulation Approach to the Properties of Polyimides. WAXD patterns demonstrate that the small size of hexagonal carbon layers, which referring to graphitic sheetlike structures are the basic structure units in the carbon materials prepared under 800 °C. These graphitic sheetlike structures are random stacked and random oriented. In addition, the improvement of layer orientation was retarded during the solid-state carbonization. Therefore, the graphitization ability of the resultant carbon membranes should be somewhat predetermined by the flatness of the precursor molecules and their in-plane orientation along the film surface.[28,29]

Since these polyimides have the same diamine groups, the difference of dianhydride structures may dominate the dissimilarity of polyimide properties. Moreover, the two aromatic rings in dianhydride should play important roles in the graphitization process. Consequently, we consider that it is reasonable to express the flatness of polyimide molecules using the dihedral angle between the two aromatic rings in dianhydride structure. The three dimensions structures for these polyimide units in this study were built using Cerius[2] software and illustrated in Figure 1. Since the polyimides will be carbonized at above 500 °C, the temperature of simulation process is set to 500 °C. To obtain simulated structures at the global minimization state, these structures were initially relaxed through molecular dynamics, followed by optimization using molecular mechanics. The dihedral angles between the two aromatic rings in dianhydride structures were directly measured in the software and listed in Table 3. Accordingly, the sequence of molecular flatness should be BPDA-DAI > BTDA-DAI > ODPA-DAI > 6FDA-DAI. We can assume that the two aromatic rings in BPDA-DAI or BTDA-DAI are much easier to transit to the conjugated graphite sheets, compared with those in ODPA-DAI and 6FDA-DAI polyimide.

In-plane orientation of polyimides is defined as the degree of the chain axis orientation parallel to the film plane, namely the anisotropy in the edge view.[30] A certain extent of in-plane orientation probably is brought by the dimensional change along the thickness direction during solvent evaporation of polyimide solution in the casting process and densification of polyimide films in heat treatment. Normally, the in-plane orientation could be quantitatively estimated by means of WAXD,[31,32] birefringence measurement with a refractometer or an optical waveguide,[33] and reflection infrared spectroscopy.[34] Normally, birefringence measurements used a prism coupler. The refractive index of the films was measured in transverse electric and transverse magnetic modes by choosing the appropriate polarization of the incident laser beam. WAXD tests also need combine reflection and transmission modes. However, it was difficult to get a good coupling mode pattern for films of >20 μm thick.[35] Since the thickness of our films is controlled around 50 μm in the present work, we utilized RMMC simulation results and conoscopic observation to demonstrate the degree of in-plane orientation of polyimide films indirectly. According to the report of Hasegawa et al.,[30] the degree of in-plane orientation is related to the polymer chain linearity, the interchain interaction, and the molecular chain mobility. The simulated properties, such as mean-squared end-to-end distance, molar stiffness, and intrinsic viscosity, for four polyimides with same number of repeated units, are also listed in Table 3. It is obvious that the order of mean-squared end-to-end distance and molar stiffness for such four polyimides all are BPDA-DAI > BTDA-DAI > ODPA-DAI > 6FDA-DAI. It means that the BPDA-DAI polyimide has the best linearity. This is may be explainable from the flexible linkages (carboxide group in BTDA, oxide group in ODPA, and hexafluoropropane group in 6FDA) in other polyimide main chains which can lower considerably the chain linearity and stiffness. In addition, the bulky side groups not only prevent the polymer chains from dense stacking but also hinder the interchain motion during film formation. Consequently, the sequence of intrinsic viscosities is also followed by BPDA-DAI > BTDA-DAI > ODPA-DAI > 6FDA-DAI. Table 3 also shows the phase shift of polarized light through polyimide films. The result indicates that the phase shift is the most obvious after the laser light passing through BPDA-DAI polyimide films. In other words, the BPDA-DAI polyimide shows the highest degree of in-plane orientation. Other three polyimides only show a slight degree of in-plane orientation, but the sequence is the same as our simulated results: BPDA-DAI > BTDA-DAI > ODPA-DAI > 6FDA-DAI.

TABLE 4: Gas Permeation of Carbon Membranes from 550 °C Pyrolysis (10 atm and 35 °C)

	permeability (barrer)				ideal selectivity	
	O_2	N_2	CH_4	CO_2	O_2/N_2	CO_2/CH_4
CM-BTDA-550	578	128	93.7	1923	4.5	21
CM-ODPA-550	404	85.8	73.4	1321	4.7	18
CM-BPDA-550	509	112	82	1564	4.5	19
CM-6FDA-550	909	193	174	4800	4.7	28

To integrate the above two sequences of flatness and in-plane orientation for polyimides, we could predict that the degree of graphitization would be the same order as follows: BPDA-DAI > BTDA-DAI > ODPA-DAI > 6FDA-DAI, when pyrolysis temperature reaches above 700 °C. A higher degree of graphitization means more ordered membrane structures, which lead to better efficiency to distinguish gas penetrants with different molecular sizes. Consequently, we may anticipate that the polyimides with more coplanar structure and in-plane orientation chains will produce better gas separation properties for carbon membranes pyrolyzed at high temperatures.

3.4. Gas Permeation through Carbon Membranes Pyrolized under 550 °C. The gas permeabilities and ideal selectivities of O_2, N_2, CO_2, and CH_4 through carbon membranes carbonized at 550 °C under a vacuum environment are summarized in Table 4. Carbon membranes pyrolyzed at 550 °C exhibited much higher gas permeabilities as compared to the polyimides list in Table 2. To compare the four carbon membranes from different polyimides with each other, the gas permeabilities almost follow the sequence of polyimides' FFV, except for CM-BTDA-550. This result is consistent with Park et al. conclusion that the FFV of polymer precursors is an important factor to determine the performance of resultant carbon membranes. It is expected that polymer precursors with a small FFV will produce carbon membranes with a denser structure.

However, the exception of CM-BTDA-550 reveals another possible factor to affect the gas permeability of carbon membranes. The tremendous increase in CM-BTDA-550's permeability indicates a more open molecular matrix in the resultant carbon membranes than in the original polyimides. Since the opening structure of carbon membranes is mainly resulted from the evaporation of the gas products of polyimide decomposition, the CM-6FDA-550 which has the largest weight loss during pyrolysis process may recreate more interstitial space and results in the highest gas permeability. Moreover, the TGA result implies that BTDA-DAI polyimide has the lowest thermal stability among four polyimides, and its weight loss is also larger than the BPDA-DAI polyimide. Thus, the low thermal stability and more weight loss could be reasons why the gas permeabilities of CM-BTDA-550 are higher than those of carbon membranes from ODTA-DAI and BPDA-DAI polyimides which have a higher FFV. Therefore, a conclusion could be obtained that both the thermal stability and FFV of precursors play important roles affecting the gas permeabilities of carbon membranes at low pyrolysis temperatures.

Interestingly, these carbon membranes also present higher ideal gas selectivities than polyimides, especially for CO_2/CH_4. The improvement of gas separation performance results from the change of gas transport mechanism through these membranes. In polyimide films, gas transports though film by the solution−diffusion mechanism, where thermally activated motions of chain segments generate transient gaps larger than the diffusing gas; thus, the diffusive jumps occur. Therefore, the gas selective factors are related with the *d* spacing and flexibility of polymer chains. However, carbon membranes are highly porous and their structure is inflexible. We assume two kinds of pores in carbon membranes. According to the above discussion, the carbon membranes pyrolyzed at low temperatures retain similar amorphous structure as its precursor. The ultramicropore dimension should be close to the *d* spacing of polyimides (5−6 Å). The gas selective factors will be determined by the dimension and shape of the ultra-micropores. The larger micropores (>10 Å), which are produced from evaporation of decomposition products, improve the gas permeability through carbon membranes, since the larger pores connect the ultra-micropores with each other.

If the pore size is in the region of 5−10 Å, selective surface flow is expected to take place.[36] CO_2 is a more condensable and adsorptive gas compared with CH_4, O_2, and N_2. Therefore, the gas pairs (CO_2/CH_4) show more obvious increases in gas selectivity than the O_2/N_2 pair. In addition, the CM-6FDA-550 exhibits higher gas selectivity of CO_2/CH_4 than other carbon membranes. The possible reason is that more gas products from the decomposition of precursor induce more micropores in CM-6FDA-550. These micropores not only make more ultra-micropores including in gas transport channels by connecting them with each other but also increase the pore surface area which is benefit in selective surface flow. This assumption is confirmed by the pore volume measurements from CO_2 adsorption isotherm, as shown in Figure 5. The pore volume of CM-6FDA-550 and CM-BPDA-550 was calculated using the Dubinin−Astakhov equation, $W = W_0 \exp[(A/E)^n]$, where W is the pore volume, E is the characteristic energy of sorption, and W_0 is the limiting pore volume larger than adsorbates. A is related to the CO_2 critical pressure P_s and test pressure P, $A = RT \ln(p_s/p)$ and n is 2 for microcarbon structure.[37] The pore volume of CM-6FDA-550 is 0.455 cm^3/g, and the pore volume of CM-BPDA-550 is 0.318 cm^3/g.

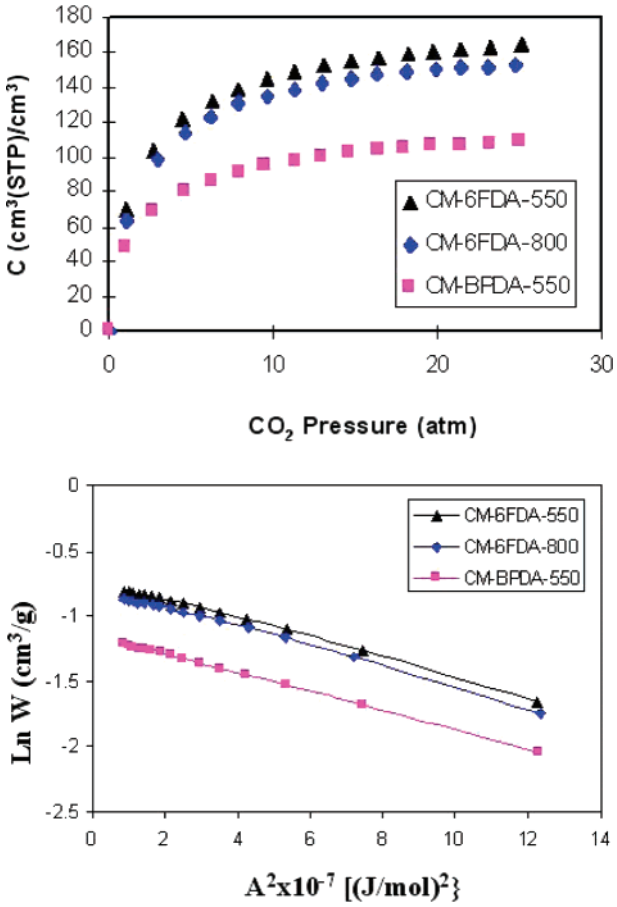

Figure 5. CO_2 adsorption isotherm at 35 °C and the typical Dubinin−Astakhov plots for carbon membranes.

TABLE 5: Gas Permeation of Carbon Membranes from 800 °C Pyrolysis (10 atm and 35 °C)

	permeability (barrer)				ideal selectivity	
	O_2	N_2	CH_4	CO_2	O_2/N_2	CO_2/CH_4
CM-BTDA-800	144	16.3	4.75	500	8.8	105
CM-ODPA-800	116	14.9	6.4	344	7.8	54
CM-BPDA-800	118	13.8	4.3	353	8.5	82
CM-6FDA-800	160	23	8.2	580	6.9	71

3.5. Gas Permeation through Carbon Membranes Pyrolyzed under 800 °C. All the gas permeabilities decrease and selectivities increase with the final pyrolysis temperature up to 800 °C, as listed in Table 5. These carbon membranes exhibited lower gas permeabilities but better gas selectivities, as compared to the carbon membranes pyrolyzed under 550 °C. As confirmed by WAXD data, higher pyrolysis temperature induces the amorphous carbon more ordered and tighter structure. On the other hand, the pore volume of the carbon membrane only decreases a little when pyrolysis temperature increases, as shown in Figure 5. The possible reason is that the graphitization mainly narrows the size of ultra-micropores. Some pores may be completely closed during pyrolysis, so that the number of channels actually connecting both face of the membranes is reduced. As the result, the gas permeabilities are reduced but selectivities are improved. To compare the gas permeabilies among four carbon membranes from different precursors, we find that CM-BTDA-800 and CM-6FDA-800 still hold higher gas permeability than CM-ODPA-800 and CM-BPDA-800. However, the difference between gas permeabilities of CM-ODPA-800 and CM-BPDA-800 is not obvious. It may well be the case that thermal stability is a more important factor to

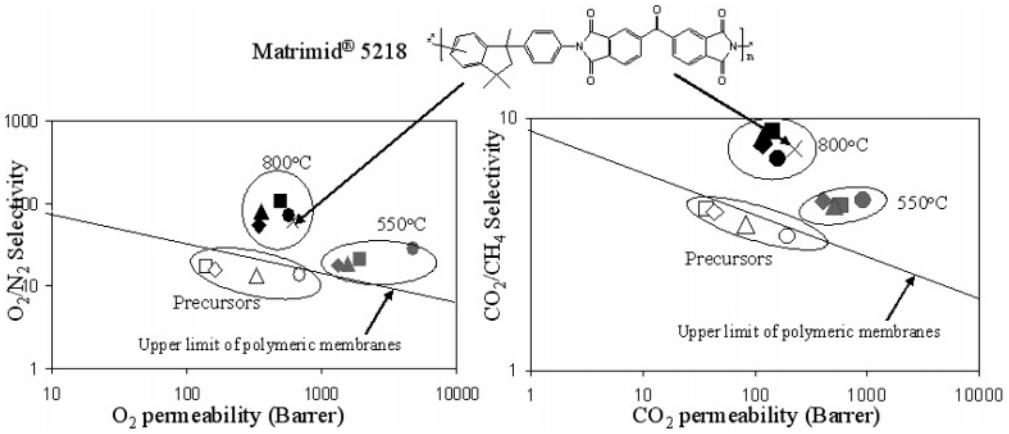

Figure 6. Tradeoff relationships of O_2/N_2 and CO_2/CH_4: (□) BTDA; (◇) ODPA; (△) BPDA; (○) 6FDA.

decide the gas permeabilities of carbon membrane compared with FFV effects when pyrolysis temperature is high. In other words, thermal stability at the high pyrolysis temperature determines the number of bigger pores.

When the selective pore dimension is below 5 Å, which is close to gas molecular sizes, the molecular sieving mechanism should dominate the gas transport through membranes. Smaller dimensions of pore structures restrict more degrees of rotation freedom of gas penetrants. Consequently, the gas selectivities increase when carbon membranes are prepared at high pyrolysis temperatures. Additionally, the increment of gas selectivity for CO_2/CH_4 pair is more distinct, since it has bigger size difference than the O_2/N_2 pair. However, the degrees of the increment in gas selectivity vary among the four polyimides. CM-BTDA-800 and CM-BPDA-800 show more increment in gas selectivity than CM-ODPA-800 and CM-6FDA-800. This tendency is consistent with our previous anticipation about the sequence of graphitization for four polyimides. As compared with ODPA-DAI and 6FDA-DAI polyimides, BTDA-DAI and BPDA-DAI polyimides show better molecular flatness and chain in-plane orientation. Thus, the carbon membranes derived from these two polyimides should have more graphitic structure, which means more ordered structure and narrow pore dimension distribution. Hence, it is reasonable that CM-BTDA-800 and CM-BPDA-800 demonstrate better gas separation properties than CM-ODPA-800 and CM-6FDA-800.

3.6. A Comparison of Gas Separation Performance with the Traditional Upper Limit Bound. Figure 6 shows the tradeoff line between selectivity and permeability for O_2/N_2 and CO_2/CH_4 pairs. From this figure, we can understand how much the performance of polyimide membranes can be improved when they are properly pyrolyzed. Moreover, we can advise which polyimide as the precursor of carbon membranes should be chosen under respective pyrolysis conditions. Generally, high FFV and low thermal stable polyimides, such as 6FDA−polyimide, are good candidates to prepare carbon membranes under low pyrolysis temperatures, if the productivity is considered as the main destination. If the distance to the tradeoff line is an indicator of the preferred gas separation efficiency, then carbon membranes pyrolyzed from the BTDA−polyimide under high temperatures is the best choice.

Two aromatic polyimide-type precursors containing BTDA group are commercially available for carbon membranes fabrication; they are Matrimid and BTDA-TDI/MDI (P84). However, only Matrimid polyimide contains the indan group like BTDA-DAI polyimide. Therefore, in Figure 6, the permeation properties of CM-BTDA-800 are compared with the carbon membranes derived from Matrimid polyimide which previously prepared by Tin et al.[16] under the same pyrolysis conditions. Carbon membranes produced from the Matrimid precursor appear to have inferior separation performance to BTDA-DAI derived carbon membranes possibly because of the following reasons. Even though both Matrimid and BTDA-DAI polyimide have indan structures, they locate differently. The indan structure in Matrimid is incorporated into the main chain, but BTDA-DAI one can be looked as a side group. Since the indan structure is not a coplanar structure, it actually destroys the molecular flatness of Matrimid polyimide. Moreover, the indan structure in the main backbone increase the flexibility of the main chain. As a result, the degree of graphitization of Matrimide polyimide should be less than that of the BTDA-DAI polyimide, and the carbon membrane prepared from the latter exhibits better gas separation properties than from the former.

4. Conclusion

Carbon membranes derived from four polyimides with different chemical structures were prepared at 550 and 800 °C. It was found that the chemical structure of polyimides significantly affected the final gas separation properties of the carbon membranes.

(1) When the pyrolysis temperature is 550 °C, higher FFV and low thermal stability of polyimides led to high gas permeability of carbon membranes. Since the selective surface flow will play a significant role when condensable gases pass though carbon membranes pyrolyzed at the low temperature, higher FFV and low thermal stability of polyimides also produce better gas selectivity of carbon membranes.

(2) Simulation results indicate that different chemical structures bring polyimides different chain flatness and in-plane orientation which affect the degree of graphitization of carbon membranes pyrolysis at high temperatures. The carbon membranes from BPDA-DAI and BTDA-DAI polyimides with good chain flatness and in-plane orientation show good gas selectivities. Furthermore, the carbon membranes from low thermal stable 6FDA-DAI and BTDA-DAI polyimides still provide considerable gas permeability.

(3) Carbon membranes derived from the BTDA-DAI precursor have superior separation performance to those derived from Matrimid. This is due to the fact that BTDA-DAI polyimide has the indan group as a side group, while Matrimid has it in the main chain. The former has a higher degree of chain flatness and in-plane orientation than the latter.

Acknowledgment. The authors thank A*Star and NUS for funding this research with Grants R-279-000-113-304 and

R-279-000-108-112, respectively. Special thanks are due to Ms. Pei Shi Tin, Ms. May May Teoh, and Mr. Jun Ying Xiong for their useful discussion and to Dr. Songlin Liu and Mr. K. Goto (Mitsui) for their assistance on materials synthesis.

References and Notes

(1) Paul, D. R.; Yampol'skii, Y. P. *Polymeric Gas Separation Membranes*; CRC Press: Boca Raton, FL, 1994.

(2) Matsuura, T. *Synthetic Membranes and Membrane Separation Processes*; CRC Press: Boca Raton, FL, 1994.

(3) Ho, W. S. W.; Sirkar, K. K. *Membrane Handbook*; Van Nostrand Reinhold: New York, 1992.

(4) Stern, S. A. Polymers for gas separations: the next decade. *J. Membr. Sci.* **1994**, *94*, 1.

(5) Hirayama, Y.; Yoshinaga, T.; Kusuki, Y.; Ninomiya, K.; Sakakibara, T.; Tamari, T. Relation of gas permeability with structure of aromatic polyimides I. *J. Membr. Sci.* **1996**, *111*, 169.

(6) Ayala, D.; Lozano, A. E.; Abajo, J. D.; Perez, C. G.; Campa, J. G.; Peinemann, K. V.; Freeman, B. D.; Prabhakar, R. Gas separation properties of aromatic polyimides. *J. Membr. Sci.* **2003**, *215*, 61.

(7) Baer, E.; Hu, Y. S.; Liu, R. Y. F.; Schiraldi, D. A.; Hiltner, A. Barrier properties of polyesters——relationship between diffusion and solid-state structure. *Polym. Mater. Sci. Eng.* **2003**, *89*, 19.

(8) Robeson, L. M. Correlation of separation factor versus permeability for polymeric membranes. *J. Membr. Sci.* **1991**, *62*, 165.

(9) Freeman, B. D. Basis of permeability/selectivity tradeoff relations in polymeric gas separion membranes. *Macromolecules* **1999**, *32*, 375.

(10) Koros, W. J.; Mahajan, R. Pushing the limits on possibilities for large scale gas separation: which strategies? *J. Membr. Sci.* **2000**, *175*, 181.

(11) Saufi, S. M.; Ismail, A. F. Fabrication of carbon membranes for gas separation—a review. *Carbon* **2004**, *42*, 241.

(12) Geiszler, V. C.; Koros, W. J. Effects of polyimide pyrolysis conditions on carbon molecular sieve membrane properties. *Ind. Eng. Chem. Res.* **1996**, *35*, 2999.

(13) Kusuki, Y.; Shimazaki, H.; Tanihara, N.; Nakanishi, S.; Toshinaga, T. Gas permeation properties and characterization of asymmetric carbon membranes prepared by pyrolyzing asymmetric polyimide hollow fiber membrane. *J. Membr. Sci.* **1997**, *134*, 245.

(14) Okamoto, K.; Kawamura, S.; Yoshino, M.; Kita, H.; Hirayama, Y.; Tanihara, N.; Kusuki, Y. Olefin/parafin separation through carbonized membranes derived from an asymmetric polyimide hollow fiber membrane. *Ind. Eng. Chem. Res.* **1999**, *38*, 4424.

(15) Tin, P. S.; Chung, T. S.; Hill, A. J. Advanced fabrication of carbon molecular sieve membranes by nonsolvent pretreatment of precursor polymers. *Ind. Eng. Chem. Res.* **2004**, *43*, 6476.

(16) Tin, P. S.; Chung, T. S.; Kawi, S.; Guiver, M. D. Novel approaches to fabricate carbon molecular sieve membranes based on chemical modified and solvent treated polyimides. *Microporous Mesoporous Mater.* **2004**, *73*, 151.

(17) Koresh, J. E.; Soffer, A. Study of molecular sieve carbons Part 1. Pore structure, gradual pore opening and mechanism of molecular sieving. *J. Chem. Soc., Faraday Trans.* **1980**, *76*, 2457.

(18) Suda, H.; Haraya, K. Alkene/alkane permselectivities of a carbon molecular sieve membrane. *Chem. Commun.* **1997**, 93.

(19) Hayashi, J.; Yamanoto, M.; Kusakabe, K.; Morooka, S. Effect of oxidation on gas permeation of carbon molecular sieving membranes based on BPDA-pp¢ODA polyimide. *Ind. Eng. Chem. Res.* **1997**, *36*, 2134.

(20) Park, H. B.; Kim, Y. K.; Lee, J. M.; Lee, S. Y.; Lee, Y. M. Relationship between chemical structure of aromatic polyimides and gas permeation properties of their carbon molecular sieve membranes. *J. Membr. Sci.* **2004**, *229*, 117.

(21) Tamai, S.; Kamada, J.; Goto, K.; Yamaguchi, A. Preparation and properties of novel aromatic polyimides from 5,7-diamino-1,1,4,6-tetramethylindan and aromatic tetracarboxylic dianhydrides. *High Perform. Polym.* **2001**, *13*, 173.

(22) Tamai, S.; Kamada, J.; Ono, T.; Goto, K.; Yamaguchi, Synthesis of photoreactive polyimide having indan structure. *J. Polym. Sci., Part A: Polym. Chem.* **2002**, *40*, 423.

(23) Liu, S. L.; Chng, M. L.; Chung, T. S.; Goto, K.; Tamai, S.; Pramoda, K. P.; Tong, Y. J. Gas-transport properties of indan-containing polyimides. *J. Polym. Sci., Part B: Polym. Phys.* **2004**, *42*, 2769.

(24) Park, J. Y.; Paul, D. R. Correlation and prediction of gas permeability in glassy polymer membrane materials via a modified free volume based group contribution method. *J. Membr. Sci.* **1997**, *125*, 23.

(25) *Cerius*^{2} *Simulation Tool User's Reference, Molecular Simulations Software for Material Science*; Molecular Simulation Inc.: San Diego, CA, 1996.

(26) Lin, W. H.; Vora, R. H.; Chung, T. S. Gas transport properties of 6FDA-durene/pPDA copolyimides. *J. Polym. Sci., Part B: Polym. Phys.* **2000**, *38*, 2703.

(27) Kim, T. H.; Koros, W. J.; Husk, G. R.; O'brien, K. C. Relationship between gas separation properties and chemical structure in a series of aromatic polyimides. *J. Membr. Sci.* **1988**, *37*, 45.

(28) Hatori, H.; Yamada, Y.; Shiraishi, M. In-plane orientation and graphitization of polyimide films. *Carbon* **1992**, *30*, 763.

(29) Inagaki, M.; Sato, M.; Takeichi, M.; Yoshida, A.; Hishiyama, Y. Effect of constraint during imidization of polyamic acid films on graphitizability of resultant carbon films. *Carbon* **1992**, *30*, 903.

(30) Hasegawa, M.; Matano, T.; Shindo. Y.; Sugimura, T. Spontaneous molecular orientation of polyimide induced by thermal imidization. 2. in-plane orientation. *Macromolecules* **1996**, *29*, 7897.

(31) Arnold, F. E., Jr.; Shen, D.; Lee, C. J.; Harris, F. H.; Cheng, S. Z. D.; Lau, S. F. Organo-soluble segmented rigid-rod polyimide films. Part 4.—Anisotropic structure and properties. *J. Mater. Chem.* **1993**, *3*, 353.

(32) Factor, B. J.; Russell, T. P.; Toney, M. F. Grazing incidence X-ray scattering studies of thin films of an aromatic polyimide. *Macromolecules* **1993**, *26*, 2847.

(33) Herminghaus, S.; Boese, D.; Yoon, D. Y.; Smith, B. A. Large anisotropy in optical properties of thin polyimide films of poly(*p*-phenylene biphenyltetracarboximide). *Appl. Phys. Lett.* **1991**, *59*, 1043.

(34) Perez, M. A.; Ren, Y.; Farris, R. J.; Hsu, S. L. Characterization of PMDA-ODA Polyimide Films by External Reflectance Infrared Spectroscopy. *Macromolecules* **1994**, *27*, 6740.

(35) Ree, M.; Chu, C. W.; Goldberg, M. J. Influences of chain rigidity, in-plan orientation, and thickness on residual stress of polymer films. *J. Appl. Phys.* **1994**, *75*, 1410.

(36) Rao, M. B.; Sircar, S. Performance and pore characterization of nanoporous carbon membranes for gas separation. *J. Membr. Sci.* **1996**, *110*, 109.

(37) Suda, H.; Haraya, K. Gas permeation through micropores of carbon molecular sieve membranes derived from Kapton polyimide. *J. Phys. Chem. B* **1997**, *101*, 3988.